High-Pressure Structures of Disilane and Their Superconducting Properties

José A. Flores-Livas,[1] Maximilian Amsler,[2] Thomas J. Lenosky,[3] Lauri Lehtovaara,[1] Silvana Botti,[1] Miguel A. L. Marques,[1,*] and Stefan Goedecker[2,†]

[1]*Université de Lyon, F-69000 Lyon, France, and LPMCN, CNRS, UMR 5586, Université Lyon 1, F-69622 Villeurbanne, France*
[2]*Department of Physics, Universität Basel, Klingelbergstrasse 82, 4056 Basel, Switzerland*
[3]*C8 Medisensors, Los Gatos, California 95032, USA*

(Received 16 November 2011; published 14 March 2012)

A systematic *ab initio* search for low-enthalpy phases of disilane (Si_2H_6) at high pressures was performed based on the minima hopping method. We found a novel metallic phase of disilane with *Cmcm* symmetry, which is enthalpically more favorable than the recently proposed structures of disilane up to 280 GPa, but revealing compositional instability below 190 GPa. The *Cmcm* phase has a moderate electron-phonon coupling yielding a superconducting transition temperature T_c of around 20 K at 100 GPa, decreasing to 13 K at 220 GPa. These values are significantly smaller than previously predicted T_c's for disilane at equivalent pressure. This shows that similar but different crystalline structures of a material can result in dramatically different T_c's and stresses the need for a systematic search for a crystalline ground state.

DOI: 10.1103/PhysRevLett.108.117004 PACS numbers: 74.70.Ad, 61.66.Fn, 74.10.+v, 74.62.Fj

Superconductivity in elemental hydrogen was predicted by Ashcroft [1] already in 1968. More recently, and with the use of novel theoretical techniques [2,3], the calculated T_c was estimated to be as high as 240 K at pressures of around 450 GPa in molecular hydrogen [4]. Furthermore, very recent studies of atomic hydrogen found a transition temperature of 356 K at 500 GPa [5] and T_c's of above 600 K at pressures beyond 1 TPa [5,6]. However, the synthesis of metallic hydrogen has been found to be experimentally challenging, and even at extremely high pressures (below 320 GPa) metallization has not yet been observed [7]. This is in agreement with theoretical calculations that predict the metallic transition above 400 GPa [8]—a pressure beyond the reach of current experimental capabilities.

To circumvent this problem, it was recently suggested that metallization pressures could be achieved in hydrogen-rich materials where the hydrogen is chemically ''precompressed'' [9]. Several investigations of such compounds have appeared in the literature, primarily focusing on group-IV hydrides. Calculations on phases of highly compressed silane [10–15], germane [16], and stannane [17,18] have shown the possibility of metallic phases with high T_c at moderate pressures. From the experimental point of view, silane SiH_4 has been reported to crystallize and attain metallicity above 50–60 GPa [19,20] with a superconducting behavior. However, more recent studies ascribe the observed metallicity to the formation of metal hydrides [21], and metallization of silane was found not to occur at least below 130 GPa [22].

Another hydrogen-rich compound of the same family is disilane Si_2H_6. This compound has attracted attention as a hydrogen-rich material due to its experimental availability. Moreover, in a recent theoretical study, Jin *et al.* [23] performed random searches in order to find stable structures of disilane. They reported three different structures covering a pressure range from 50 to 400 GPa. Crystallization of disilane into a metallic phase with a *P*-1 lattice was predicted to occur at 135 GPa. The T_c of this phase was predicted to be 64.6 K at 175 GPa and 80.1 K at 200 GPa. Beyond 175 GPa, the lowest enthalpy phase was found to be a cubic *Pm*-3*m* structure that reaches the remarkable superconducting transition temperature of $T_c = 139$ K at 275 GPa, a T_c much higher than any other predicted transition temperature of group-IV hydrides. Unfortunately, these results have not been experimentally confirmed.

In this Letter, we report on our investigations of the disilane system under pressure by using the recently developed minima hopping method (MHM) [24,25] for the prediction of low-enthalpy structures. This method has been successfully used for global geometry optimization in a large variety of applications [26–30]. Given only the chemical composition of a system, the MHM aims at finding the global minimum on the enthalpy surface while gradually exploring low-lying structures. Moves on the enthalpy surface are performed by using variable cell shape molecular dynamics with initial velocities approximately chosen along soft mode directions. The relaxations to local minima are performed by the fast inertia relaxation engine [31] by taking into account both atomic and cell degrees of freedom.

We performed simulations for cells containing 1, 2, and 3 f.u. of disilane Si_2H_6 under several different pressures between 40 and 400 GPa. The initial sampling of the enthalpy surface was carried out by employing the MHM together with Lenosky's tight-binding scheme [32], extended to include hydrogen. The most promising candidate

structures found during the initial sampling were further studied [33,34] at the density-functional theory level by using the Perdew-Burke-Ernzerhof exchange-correlation functional [35] and norm-conserving Hartwigsen-Goedecker-Hutter pseudopotentials [36]. The plane-wave cutoff energy was set to 1400 eV, and Monkhorst-Pack k-point meshes [37] with grid spacing denser than $2\pi \times 0.025$ Å were used, resulting in total energy convergence to better than 1 meV/atom. Finally, in order to confirm that the tight-binding scheme was able to sufficiently sample the enthalpy surfaces, we performed MHM simulations for selected pressures of 100, 200, 280, and 320 GPa at the density-functional theory level.

In Fig. 1, the enthalpy of the different phases found in our MHM simulations are shown with respect to decomposition towards elemental silicon and hydrogen. At pressures above 280 GPa, the Pm-3m phase is favored, competing with several other structures reported by Jin *et al.* [23]. In addition to the structures reported in Ref. [23], our simulations revealed another low-lying phase with P-1 symmetry [Fig. 2(b)]. However, all these structures lie in a very small enthalpy range, which is within our numerical precision. In fact, taking into account the zero-point vibrational energies might easily change the energy ordering, and in general one can expect that at a finite temperature the competing low-enthalpy phases will be present as an admixture.

As seen also in Fig. 1, crystalline disilane is enthalpically unstable towards decomposition to elemental silicon and hydrogen below 95 GPa. A decomposition to silane SiH_4 together with elemental silicon and hydrogen is enthalpically possible up to pressures of 190 GPa. This compositional instability could pose challenges en route to synthesization of crystalline disilane, depending on barrier heights and on the dynamics of the decomposition.

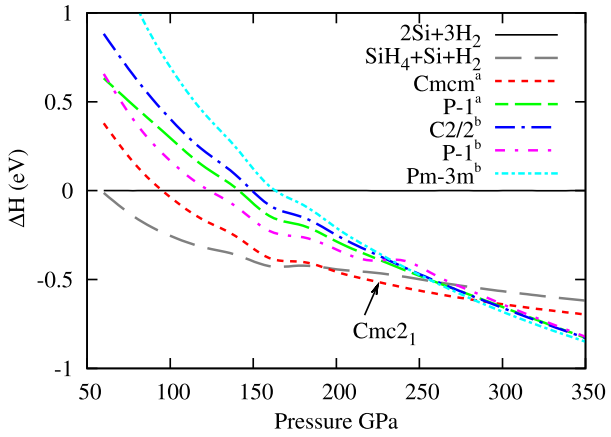

FIG. 1 (color online). Enthalpy per formula unit of disilane as a function of pressure with respect to elements in their solid form $2\mathrm{Si}(s) + 3\mathrm{H}_2(s)$. The decomposition enthalpies were computed from the predicted structures of hydrogen ($P6_3/m$, $C2/c$) [44], high-pressure phases of silicon ($P6/mmm$, $P6_3/mmc$, $Fm-3m$) [45,46], and silane ($Fdd2$, $I4_1/a$, $Pbcn$) [10,15]. The disilane structures with superscripts a and b are from this work and from Ref. [23], respectively. The dynamical instability towards the $Cmc2_1$ phase is indicated by the arrow.

Yet another low-enthalpy metallic phase of disilane was found during our MHM simulations [see Fig. 2(a)]. It belongs to the $Cmcm$ space group and is the lowest enthalpy structure up to 280 GPa. We would like to stress that the enthalpy difference between the $Cmcm$ phase and the previously proposed P-1 phase close to 200 GPa is relatively large, so that a change in the enthalpy ordering due to the zero-point vibrational energy is very unlikely. At 200 GPa, its conventional cell parameters are $a = 7.965$ Å, $b = 2.705$ Å, and $c = 4.728$ Å, with one silicon atom occupying the 8e crystallographic site at $(0.141, 0, 0)$ and three hydrogen atoms occupying 8g, 8g, and 8f sites at coordinates $(0.293, 0.173, 0.250)$, $(0.086, 0.302, 0.250)$, and $(0, 0.311, 0.895)$, respectively. The hydrogen atoms are embedded into a framework of fivefold coordinated silicon atoms. The average silicon-silicon bond length is 2.28 Å, and each silicon atom is surrounded by six hydrogen atoms at a mean distance of 1.52 Å.

We further characterized the $Cmcm$ structure by performing calculations of the phonon spectrum, the electron-phonon coupling, and the superconducting transition temperature T_c. The phonon spectrum and the electron-phonon matrix elements were obtained from density-functional perturbation theory [38]. The spectral function $\alpha^2F(\omega)$ was integrated over the Fermi surface by applying the tetrahedron technique. Convergence of the above quantities was ensured by a $16 \times 16 \times 16$ Monkhorst-Pack k-point sampling and a $4 \times 4 \times 4$ q-point sampling for the phonon wave vectors. The above settings result in T_c's converged to less than 1 K. The phonon dispersion

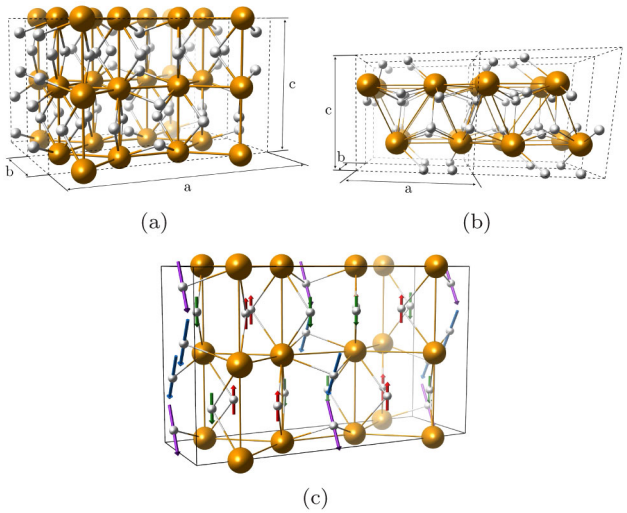

FIG. 2 (color online). The crystal structures of (a) the $Cmcm$ phase at 200 GPa and (b) the P-1 phase at 300 GPa. The eigendisplacements which lead from the $Cmcm$ structure to the $Cmc2_1$ structure are visualized by arrows in (c).

was obtained by Fourier interpolating the computed dynamical matrices.

The phonon band dispersion of the *Cmcm* phase at 200 GPa can be seen in the left panel of Fig. 3, while the partial phonon density of states is shown in the right panel. As expected, the low frequencies (< 700 cm^{-1}) are dominated by the vibrations of the silicon framework, whereas the high end of the spectrum extending up to 2300 cm^{-1} is solely due to the light hydrogen atoms. We found the structure to be dynamically stable up to 220 GPa. However, if the pressure is increased beyond 225 GPa, a dynamical instability arises. The phonon band dispersion at 230 GPa can be found in the Supplemental Material [39]. It shows an imaginary (plotted as negative) frequency at the Γ point, indicating an unstable phonon mode. Following the eigendisplacements of this mode, which are shown in Fig. 2(c), and then performing a full relaxation of the structure leads to another unreported stable structure with $Cmc2_1$ symmetry. Compared to the *Cmcm* phase, the silicon framework remains essentially intact, while the hydrogen atoms are slightly displaced, partially breaking the symmetry. Because of the strong similarities between the *Cmcm* and the $Cmc2_1$ structures, we do not expect large differences in their phonons or superconducting properties. A similar analysis as above has been carried out following a further imaginary frequency arising at the *S* point when the pressure is increased above 260 GPa. The resulting structure found by following the corresponding eigendisplacements resulted in a structure with $P1c1$ symmetry (see the Supplemental Material for details on this structure) [39].

In order to investigate the superconducting properties of the *Cmcm* phase, we use McMillan's approximate formula for the superconducting transition temperature $T_c = \frac{\Omega_{\log}}{1.2} \exp[-\frac{1.04(1+\lambda)}{\lambda-\mu^*(1+0.62\lambda)}]$ [40,41]. McMillan's formula requires the superconducting properties as the weighted average of the phonon frequencies $\Omega_{\log}$, λ, which is an average of the electron-phonon interaction, and the dimensionless Coulomb pseudopotential μ^* [39]. These quantities were calculated from the Eliashberg spectral function $\alpha^2F(\omega)$, which was obtained from *ab initio* calculations performed with the ABINIT code [33,34]. In the right panel of Fig. 3, the solid lines represent the Eliashberg spectral function of the *Cmcm* phase at 200 GPa. It has three main features: (i) low optical modes of the silicon framework, (ii) two intense hydrogen peaks around 1500 and 1600 cm^{-1}, and (iii) high frequency modes of hydrogen around 2000 cm^{-1}.

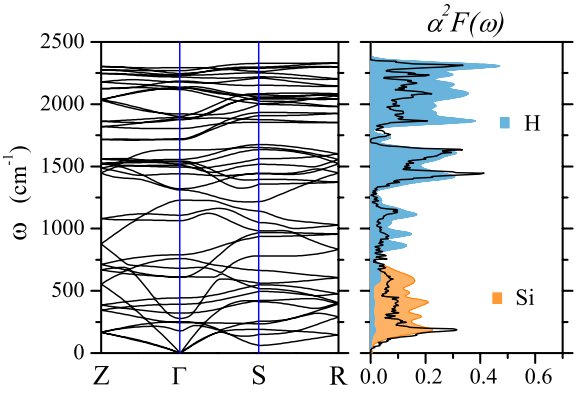

FIG. 3 (color online). Left: Phonon band dispersion of the *Cmcm* structure at 200 GPa. Right: Calculated Eliashberg spectral function $\alpha^2F(\omega)$ (solid line) and phonon partial density of states (yellow, silicon; blue, hydrogen).

The superconducting properties of the *Cmcm* phase at several pressures are summarized in Table I, by using two typical values for the Coulomb pseudopotential $\mu^* = 0.1$ and $\mu^* = 0.13$. For a better comparison, we note that Jin *et al.* [23] set $\mu^* = 0.13$. By assuming the larger of those values, the superconducting transition temperature T_c is 20.1 K at 100 GPa and decreases to 13.0 K at 220 GPa. A decreasing T_c with respect to increasing pressure has been observed in other hydrogen-rich materials [19,42,43]. We should emphasize that the T_c of the *Cmcm* phase is smaller by approximately a factor of 6.5 than of the previously reported *P*-1 structure at 200 GPa and that the *Cmcm* phase is the lowest enthalpy phase. This raises serious doubts if high-T_c superconductivity will ever be achieved in silane materials under reasonable pressure.

Furthermore, the superconducting properties of the *Cmcm* phase are strongly linked to its electronic structure. In Fig. 4, the evolution of the Fermi surface is shown as a function of pressure. Three states cross the Fermi surface. The first (magenta) and the second (yellow) states cover an important portion of the Brillouin zone that overlaps in the edged of the Brillouin zone and remain nearly unaltered as the pressure increases, whereas the third (cyan) changes substantially. The contribution of this third state to the Fermi surface consists of spherical regions near the Γ point. This band connects two main portions of the Fermi surface. Therefore, we can expect high superconducting values for low pressures: $\lambda = 0.84$ and $\Omega_{\log} = 480$ with a T_c of 20 K at 100 GPa. However, as the volume of the structure decreases with increasing pressure, this sphere-like feature of the Fermi surface is abruptly reduced.

TABLE I. Superconducting properties of the *Cmcm* phase at different pressures. The transition temperatures were calculated by using Allen-Dynes modified McMillan's formula (see Supplemental Materials for details [39]).

Pressure			T_c (K)	
(GPa)	λ	$\Omega_{\log}$	$\mu^* = 0.1$	$\mu^* = 0.13$
100	0.84	478	24.6	20.2
140	0.68	553	17.9	13.5
160	0.66	556	16.7	12.4
200	0.68	501	16.2	12.2
220	0.76	384	16.1	12.7

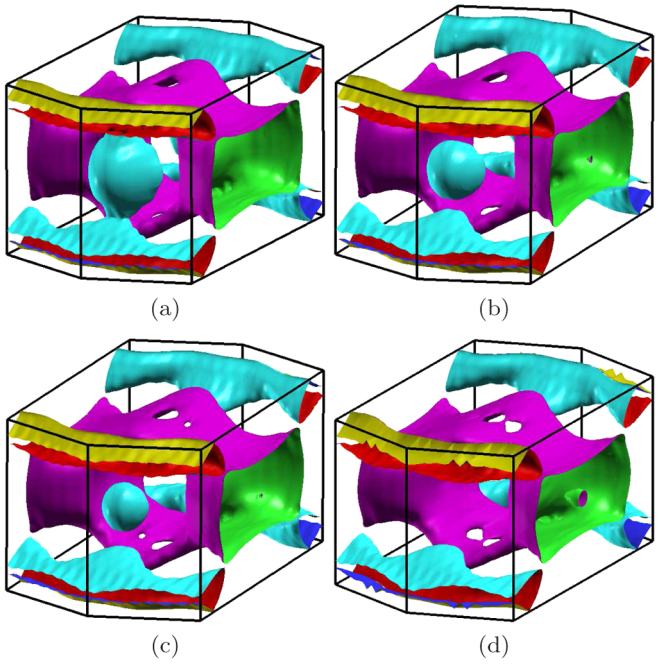

FIG. 4 (color online). Fermi surface of the *Cmcm* phase at several pressures: (a) 100, (b) 140, (c) 160, and (d) 220 GPa [47].

Consequently, at 160 GPa the superconducting parameter λ and T_c clearly decrease, while $\Omega_{\log}$ only slightly increases: $\lambda = 0.66$, $\Omega_{\log} = 556$, and $T_c = 12.4$ K.

In conclusion, we performed a thorough investigation of the high-pressure phases of disilane by using first-principles calculations. Applying our minima hopping method to explore the potential energy surface of disilane, we found a metallic structure which is enthalpically favorable compared to the previously proposed structures of disilane. Additionally, the systematic study of the superconducting properties as a function of pressure shows that the *Cmcm* phase possesses a moderate electron-phonon coupling, leading to a superconducting transition temperature in the 10–20 K range. This result stands in sharp contrast with the structures previously proposed of disilane under pressure. Moreover, we observed that the transition temperature of the *Cmcm* structure has the tendency to decrease monotonically with applied pressure, which can be understood by the shrinking of a part of the Fermi surface. This decrease of the T_c is in agreement with most theoretical and experimental results of hydrogen-rich materials, including silane [19,42,43]. Certainly, this does not imply that superconductivity in hydrogen-rich materials is limited to relatively low values of T_c for reasonably high pressure, but our results do impose strong constraints on the possibility of high-T_c superconductors in silicon-hydrogen systems.

Furthermore, our work shows the necessity of performing thorough global geometry optimizations in order to predict accurately the physical properties of the ground state of any new material. In fact, as we have shown, different metastable structures of disilane yield superconducting transition temperatures that can differ by nearly an order of magnitude. This conclusion is clearly general; i.e., for a given stoichiometry, the actual arrangement of the atoms can affect strongly the physical properties of a material. Therefore, to obtain meaningful predictions for the ground state of a new material, fully automated structure prediction schemes, like the newly developed minima hopping method [25], should be systematically employed to investigate new material properties. Such prediction schemes are very promising and powerful tools, and we can expect that they will lead to important advances in the field of materials design.

Financial support provided by the Swiss National Science Foundation is gratefully acknowledged. S. B. acknowledges support from EU's 7th Framework Program (e-I3 contract ETSF) and MALM from the French ANR (ANR-08-CEXC8-008-01). M. A. and J. A. F.-L. acknowledge the computational resources provided by the Swiss National Supercomputing Center (CSCS) in Manno and by IDRIS-GENCI (Project No. x2011096017) in France. J. A. F.-L. acknowledges the CONACyT-México for financial support.

*miguel.marques@univ-lyon1.fr
†stefan.goedecker@unibas.ch

[1] N. W. Ashcroft, Phys. Rev. Lett. **21**, 1748 (1968).
[2] M. Lüders, M. A. L. Marques, N. N. Lathiotakis, A. Floris, G. Profeta, L. Fast, A. Continenza, S. Massidda, and E. K. U. Gross, Phys. Rev. B **72**, 024545 (2005).
[3] M. A. L. Marques, M. Lüders, N. N. Lathiotakis, G. Profeta, A. Floris, L. Fast, A. Continenza, E. K. U. Gross, and S. Massidda, Phys. Rev. B **72**, 024546 (2005).
[4] P. Cudazzo, G. Profeta, A. Sanna, A. Floris, A. Continenza, S. Massidda, and E. K. U. Gross, Phys. Rev. Lett. **100**, 257001 (2008).
[5] J. M. McMahon and D. M. Ceperley, Phys. Rev. B **84**, 144515 (2011).
[6] R. Szczęśniak and M. Jarosik, Solid State Commun. **149**, 2053 (2009).
[7] P. Loubeyre, F. Occelli, and R. LeToullec, Nature (London) **416**, 613 (2002).
[8] M. Städele and R. M. Martin, Phys. Rev. Lett. **84**, 6070 (2000).
[9] N. W. Ashcroft, Phys. Rev. Lett. **92**, 187002 (2004).
[10] C. J. Pickard and R. J. Needs, Phys. Rev. Lett. **97**, 045504 (2006).
[11] J. Feng, W. Grochala, T. Jaroń, R. Hoffmann, A. Bergara, and N. W. Ashcroft, Phys. Rev. Lett. **96**, 017006 (2006).
[12] Y. Yao, J. S. Tse, Y. Ma, and K. Tanaka, Europhys. Lett. **78**, 37 003 (2007).
[13] X. J. Chen, J. L. Wang, V. V. Struzhkin, H. K. Mao, R. J. Hemley, and H. Q. Lin, Phys. Rev. Lett. **101**, 077002 (2008).
[14] D. Y. Kim, R. H. Scheicher, S. Lebègue, J. Prasongkit, B. Arnaud, M. Alouani, and R. Ahuja, Proc. Natl. Acad. Sci. U.S.A. **105**, 16 454 (2008).

[15] M. Martinez-Canales, A. R. Oganov, Y. Ma, Y. Yan, A. O. Lyakhov, and A. Bergara, Phys. Rev. Lett. **102**, 087005 (2009).
[16] G. Gao, A. R. Oganov, A. Bergara, M. Martinez-Canales, T. Cui, T. Iitaka, Y. Ma, and G. Zou, Phys. Rev. Lett. **101**, 107002 (2008).
[17] J. S. Tse, Y. Yao, and K. Tanaka, Phys. Rev. Lett. **98**, 117004 (2007).
[18] G. Gao, A. R. Oganov, P. Li, Z. Li, H. Wang, T. Cui, Y. Ma, A. Bergara, A. O. Lyakhov, T. Iitaka, and G. Zou, Proc. Natl. Acad. Sci. U.S.A. **107**, 1317 (2010).
[19] M. I. Eremets, I. A. Trojan, S. A. Medvedev, J. S. Tse, and Y. Yao, Science **319**, 1506 (2008).
[20] X. Chen, V. V. Struzhkin, Y. Song, A. F. Goncharov, M. Ahart, Z. Liu, H.-k. Mao, and R. J. Hemley, Proc. Natl. Acad. Sci. U.S.A. **105**, 20 (2008).
[21] O. Degtyareva, J. E. Proctor, C. L. Guillaume, E. Gregoryanz, and M. Hanfland, Solid State Commun. **149**, 1583 (2009).
[22] M. Hanfland, J. E. Proctor, C. L. Guillaume, O. Degtyareva, and E. Gregoryanz, Phys. Rev. Lett. **106**, 095503 (2011).
[23] X. Jin, X. Meng, Z. He, Y. Ma, B. Liu, T. Cui, G. Zou, and H.-k. Mao, Proc. Natl. Acad. Sci. U.S.A. **107**, 9969 (2010).
[24] S. Goedecker, J. Chem. Phys. **120**, 9911 (2004).
[25] M. Amsler and S. Goedecker, J. Chem. Phys. **133**, 224104 (2010).
[26] W. Hellmann, R. G. Hennig, S. Goedecker, C. J. Umrigar, B. Delley, and T. Lenosky, Phys. Rev. B **75**, 085411 (2007).
[27] S. Roy, S. Goedecker, M. J. Field, and E. Penev, J. Phys. Chem. B **113**, 7315 (2009).
[28] K. Bao, S. Goedecker, K. Koga, F. Lançon, and A. Neelov, Phys. Rev. B **79**, 041405 (2009).
[29] A. Willand, M. Gramzow, S. A. Ghasemi, L. Genovese, T. Deutsch, K. Reuter, and S. Goedecker, Phys. Rev. B **81**, 201405 (2010).
[30] M. Amsler, J. A. Flores-Livas, L. Lehtovaara, F. Balima, S. A. Ghasemi, D. Machon, S. Pailhès, A. Willand, D. Caliste, S. Botti, A. S. Miguel, S. Goedecker, and M. A. L. Marques, Phys. Rev. Lett. **108**, 065501 (2012).
[31] E. Bitzek, P. Koskinen, F. Gähler, M. Moseler, and P. Gumbsch, Phys. Rev. Lett. **97**, 170201 (2006).
[32] T. J. Lenosky, J. D. Kress, I. Kwon, A. F. Voter, B. Edwards, D. F. Richards, S. Yang, and J. B. Adams, Phys. Rev. B **55**, 1528 (1997).
[33] X. Gonze, G.-M. Rignanese, M. Verstraete, J.-M. Beuken, Y. Pouillon, R. Caracas, F. Jollet, M. Torrent, G. Zerah, M. Mikami, P. Ghosez, M. Veithen, J.-Y. Raty, V. Olevano, F. Bruneval, L. Reining, R. Godby, G. Onida, D. Hamann, and D. Allan, Z. Kristallogr. **220**, 558 (2005).
[34] X. Gonze, B. Amadon, P. Anglade, J. Beuken, F. Bottin, P. Boulanger, F. Bruneval, D. Caliste, R. Caracas, M. Côté, T. Deutsch, L. Genovese, P. Ghosez, M. Giantomassi, S. Goedecker, D. Hamann, P. Hermet, F. Jollet, G. Jomard, S. Leroux, M. Mancini, S. Mazevet, M. Oliveira, G. Onida, Y. Pouillon, T. Rangel, G. Rignanese, D. Sangalli, R. Shaltaf, M. Torrent, M. Verstraete, G. Zerah, and J. Zwanziger, Comput. Phys. Commun. **180**, 2582 (2009).
[35] J. P. Perdew, K. Burke, and M. Ernzerhof, Phys. Rev. Lett. **77**, 3865 (1996).
[36] C. Hartwigsen, S. Goedecker, and J. Hutter, Phys. Rev. B **58**, 3641 (1998).
[37] H. J. Monkhorst and J. D. Pack, Phys. Rev. B **13**, 5188 (1976).
[38] S. Baroni, S. de Gironcoli, A. Dal Corso, and P. Giannozzi, Rev. Mod. Phys. **73**, 515 (2001).
[39] See Supplemental Material at http://link.aps.org/supplemental/10.1103/PhysRevLett.108.117004 for details on the Allen-Dynes modified McMillan's formulation, phonon band structure, structural evolution, the evolution of $\alpha^2F(\omega)$ in pressure, and the IR or Raman activity present in the *Cmcm* structure.
[40] W. L. McMillan, Phys. Rev. **167**, 331 (1968).
[41] P. B. Allen and R. C. Dynes, Phys. Rev. B **12**, 905 (1975).
[42] D. Y. Kim, R. H. Scheicher, C. J. Pickard, R. J. Needs, and R. Ahuja, Phys. Rev. Lett. **107**, 117002 (2011).
[43] X.-F. Zhou, A. R. Oganov, X. Dong, L. Zhang, Y. Tian, and H.-T. Wang, Phys. Rev. B **84**, 054543 (2011).
[44] C. J. Pickard and R. J. Needs, Nature Phys. **3**, 473 (2007).
[45] H. Olijnyk, S. Sikka, and W. Holzapfel, Phys. Lett. A **103**, 137 (1984).
[46] S. J. Duclos, Y. K. Vohra, and A. L. Ruoff, Phys. Rev. Lett. **58**, 775 (1987).
[47] Anton Kokalj, Comput. Mater. Sci. **28**, 155 (2003). XCRYSDEN was used to plot the Fermi surfaces.